Highly Accurate Coupled Cluster Potential Energy Curves for the Benzene Dimer: Sandwich, T-Shaped, and Parallel-Displaced Configurations

ARTICLE *in* THE JOURNAL OF PHYSICAL CHEMISTRY A · OCTOBER 2004

Impact Factor: 2.69 · DOI: 10.1021/jp0469517

2 AUTHORS:

Mutasem Sinnokrot
Petroleum Institute (UAE)
13 PUBLICATIONS **2,673** CITATIONS
SEE PROFILE

Charles David Sherrill
Georgia Institute of Technology
174 PUBLICATIONS **10,308** CITATIONS
SEE PROFILE

Highly Accurate Coupled Cluster Potential Energy Curves for the Benzene Dimer: Sandwich, T-Shaped, and Parallel-Displaced Configurations

Mutasem Omar Sinnokrot and C. David Sherrill*

Center for Computational Molecular Science and Technology, School of Chemistry and Biochemistry, Georgia Institute of Technology, Atlanta, Georgia 30332-0400

Received: July 9, 2004; In Final Form: September 3, 2004

State-of-the-art electronic structure theory has been applied to generate potential energy curves for the sandwich, T-shaped, and parallel-displaced configurations of the simplest prototype of aromatic $\pi-\pi$ interactions, the benzene dimer. Results were obtained using second-order Møller−Plesset perturbation theory (MP2) and coupled-cluster with singles, doubles, and perturbative triples [CCSD(T)] with different augmented, correlation-consistent basis sets. At the MP2 level, the smallest basis set used (a modified aug-cc-pVDZ basis) underestimates the binding by ∼0.5 kcal mol^{-1} at equilibrium and by ∼1 kcal mol^{-1} at smaller intermonomer distances compared to results with a modified aug-cc-pVQZ basis (denoted aug-cc-pVQZ*). The best MP2 binding energies differ from the more accurate CCSD(T) values by up to 2.0 kcal mol^{-1} at equilibrium and by more than 2.5 kcal mol^{-1} at smaller intermonomer distances, highlighting the importance of going beyond MP2 to achieve higher accuracy in binding energies. Symmetry adapted perturbation theory is used to analyze interaction energies in terms of electrostatic, dispersion, induction, and exchange-repulsion contributions. The high-quality estimates of the CCSD(T)/aug-cc-pVQZ* potential energy curves for the benzene dimer presented here provide a better understanding of how the strength of $\pi-\pi$ interactions varies with distance and orientation of the rings and will assist in the development of approximate methods capable of modeling weakly bound $\pi-\pi$ systems.

Introduction

Aromatic $\pi-\pi$ interactions are ubiquitous in diverse areas of science and molecular engineering.[1−3] They are key noncovalent interactions influencing the tertiary structure of proteins,[4,5] the vertical base stacking in DNA,[6−9] and the intercalation of different drugs into DNA.[6] $\pi-\pi$ interactions also play a major role in stabilizing host−guest complexes[10,11] and self-assembly based on synthetic molecules[12−14] where aromatic rings provide additional structural stability.

Benzene dimer, the simplest prototype of aromatic $\pi-\pi$ interactions, has been extensively studied, both theoretically[15−20] and experimentally,[21−25] in an attempt to obtain a clear picture of the strength and directionality of $\pi-\pi$ interactions. The small binding energy of the gas-phase benzene dimer (∼2−3 kcal mol^{-1}) and the shallowness of the potential energy surface make it a challenge for both theory and experiment. Additionally, although microwave spectroscopy has provided a structure for the T-shaped configuration,[23] other configurations such as the sandwich and parallel-displaced configurations are more challenging because they lack permanent dipole moments.

In various complex chemical and biological systems, aromatic rings can be found at different orientations and distances from each other. Due to steric constraints imposed on the aromatic groups, these geometries might not correspond to the potential energy minima for $\pi-\pi$ interactions. Nevertheless, the aromatic rings might still interact favorably enough to contribute significantly to the overall stability of the system. In their notable X-ray crystallographic study of side-chain aromatic interactions in 34 high-resolution protein structures, Burely and Petsko[4] analyzed the frequency of aromatic pairs and their interaction geometry (distance and dihedral angle); they found that around 60% of aromatic side chains of phenylalanine, tyrosine, and tryptophan were involved in aromatic pairs. Aromatic rings separated by distances ranging from 4.5 to 7 Å and dihedral angles near 90° were found to be the most common. Pairwise nonbonded potential energy calculations indicated that 54% of the aromatic interactions are attractive by 1−2 kcal mol^{-1}. In a study of a larger database of 52 proteins,[5] Hunter, Singh, and Thornton examined the orientational preferences of phenylalanine side chains in proteins using crytallographically derived atomic coordinates. They observed that these interacting pairs are found in a wide range of T-shaped (edge-to-face) and parallel-displaced (offset-stacked) arrangements, but they are scattered over a wide variety of conformational space with no strongly preferred single orientation.

From the above discussion, it becomes clear that high-quality potential energy curves for prototype systems would be very helpful in better understanding how $\pi-\pi$ interactions depend on both the orientation and distance between the aromatic rings. Due to computational limitations, previous attempts to obtain ab initio potential energy surfaces for the benzene dimer[18,19,26−28] were mostly performed at the MP2 level and/or involved the use of relatively small basis sets; hence, they lack the high accuracy needed to model $\pi-\pi$ interactions reliably. Also, these curves generally estimated the binding energies only at a small set of intermonomer distances and are therefore, at best, incomplete.

Jaffe and Smith[26] used the MP2 method along with the 6-311G(2d,2p) basis set to evaluate the potential energy curves of the sandwich, T-shaped, parallel-displaced, and V-shaped

* To whom correspondence should be addressed. E-mail: sherrill@chemistry.gatech.edu.

10.1021/jp0469517 CCC: $27.50
Published on Web 10/23/2004

configurations of the benzene dimer and to determine the interconversion path of the parallel-displaced configuration. Even though the MP2 method is qualitatively correct, it tends to overestimate binding in van der Waals clusters. Also, the basis set used in these calculations is of medium size (384 basis functions) and does not contain any diffuse functions.

Špirko et al.[29] evaluated the CCSD(T) binding energies for different configurations of the benzene dimer to parametrize a nonempirical model (NEMO) intermolecular potential and then compared their theoretical structures and barriers to rotation with microwave and Raman spectral data. They noted sizable differences between theoretical and experimental predictions, especially the height of the barrier opposing the hindered internal rotation in the T-shaped geometry. In their study, these researchers computed 107 CCSD(T) single-point energies for the fitting of the NEMO potential using a modified cc-pVDZ basis with 228 basis functions. These computations are impressive, but the modified cc-pVDZ basis set used in the CCSD(T) computations is not large enough to yield highly accurate binding energies for $\pi-\pi$ systems.

Tsuzuki and co-workers[18,27] recently presented a careful study of the energy profile of the interconversion between the T-shaped and parallel-displaced configurations of the benzene dimer. Binding energies for a number of horizontal and vertical displacements were computed at the estimated CCSD(T) basis set limit for four tilt angles ($\phi = 0°$, 30°, 60°, and 90°) along the interconversion path. An aug(d,p)-6-311G** basis (384 basis functions) was used to estimate the MP2 contribution to the interaction energies. Our previous study of the benzene dimer[19] showed that the aug-cc-pVDZ basis set, which has the same number of basis functions as the aug(d,p)-6-311G** basis, is a significant $\sim$0.5−0.7 kcal mol^{-1} away from the MP2 complete basis set (CBS) limit. Furthermore, the basis set used to estimate the ΔCCSD(T) correction is of medium size (6-311G*) and lacks the diffuse functions needed to obtain more accurate values for this correction. These factors could affect the accuracy of the energy profile and the energetic ordering of the different configurations examined, especially if one considers that the interconversion barrier height is only 0.2 kcal mol^{-1}.

Instead of interconversion pathways between different configurations of the benzene dimer, our first goal is to obtain very reliable potential energy curves as a function of intermonomer distance(s) of various prototype configurations. In our previous study of the benzene dimer,[19] we computed MP2 potential energy curves as a function of intermonomer distance for the sandwich (S), T-shaped (T), and parallel-displaced (PD) configurations using the aug-cc-pVTZ basis set (828 basis functions), a much larger basis than previously used. At the equilibrium geometries, we also combined CBS MP2 binding energies (obtained using MP2−R12/A theory[30]) with a ΔCCSD(T) correction computed in a smaller basis (aug-cc-pVDZ) to estimate the CBS CCSD(T) results, which should provide binding energies accurate to a few tenths of one kcal mol^{-1}. However, no coupled-cluster potential energy curves were reported in that study because it was not feasible to obtain entire potential energy curves at the very high CBS CCSD(T) level of theory.

In this work, we seek potential curves that are very close to the ab initio limit while remaining computationally feasible. High-quality potential energy curves (PEC's) are obtained as a function of the intermonomer distance R for the S and T configurations and of R_1 and R_2 for the PD configuration (see Figure 1). At the MP2 level, PEC's are computed using correlation-consistent basis sets as large as aug-cc-pVQZ (minus

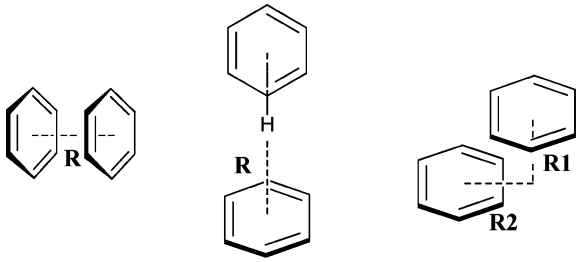

Figure 1. Sandwich, T-shaped, and parallel-displaced configurations of the benzene dimer.

g functions on carbon and *f*'s on hydrogen). The CCSD(T) potential energy curves are computed using a truncated aug-cc-pVDZ basis to produce reliable results for the ΔCCSD(T) correction, which is combined with the best MP2 values to estimate high-quality CCSD(T) potential energy curves.

The availability of reliable potential energy curves will be helpful in the calibration of molecular mechanics force field methods meant to accurately model biochemical systems exhibiting π-stacking interactions. The Lennard-Jones component of these force fields is usually fitted to ab initio gas-phase binding energies and equilibrium geometries.[31−36] In many force field calibrations, the MP2 method with polarized double-ζ or larger basis sets is used for geometry optimizations and gas-phase dimerization energy estimates.[32−36] Our present results use a considerably more reliable methodology. It is worth noting that our high-quality the benzene dimer binding energies[19] have already been used by Friesner and co-workers in calibrating their new polarizable force field.[33] In addition, these results should be useful to those developing new density functional theory methods which are meant to account for dispersion interactions.[37−39]

Theoretical Methods

All computations in this work were performed using Dunning's correlation-consistent split valence basis sets of contracted Gaussian functions.[40] Multiple polarization and diffuse functions were added to better describe the polarizability of the monomers and the delocalized nature of electrons in the benzene ring. Specifically, we used a basis (denoted aug-cc-pVDZ*) which is aug-cc-pVDZ on carbon and cc-pVDZ on hydrogen, with 336 basis functions for the benzene dimer; an aug-cc-pVTZ basis set with 828 basis functions; and an aug-cc-pVQZ basis set minus all *g* functions on carbon and all *f* functions on hydrogen (denoted aug-cc-pVQZ*) with 1128 basis functions.

Potential energy curves (PECs) as a function of intermonomer distances for the sandwich, T-shaped, and parallel-displaced configurations were computed via second order perturbation theory (MP2) with the aug-cc-pVDZ*, aug-cc-pVTZ, and aug-cc-pVQZ* basis sets. For the sandwich and T-shaped configurations, the center-to-center distance, R, was systematically varied, and for the parallel-displaced configuration both the vertical, R_1, and horizontal, R_2, distances between the centers of mass were systematically varied (see Figure 1). All calculations were performed with the recommended benzene monomer geometry of Gauss and Stanton[41] [R(C−C) = 1.3915 Å and R(C−H) = 1.0800 Å], and this geometry was not allowed to vary in the calculations. Our previous study has shown that the effect of freezing the monomer geometry is minimal on both the equilibrium geometry and binding energy of the benzene dimer.[19] The basis set superposition error (BSSE), which results from the use of an incomplete basis set, was corrected for by

the counterpoise (CP) method of Boys and Bernardi.[42] Except where otherwise noted, only CP-corrected binding energies are reported in this work. Core orbitals were constrained to remain doubly occupied in all correlated computations.

To account for the effect of triple excitations on the binding energies of the benzene dimer, CCSD(T) potential energy curves were computed using the above-mentioned aug-cc-pVDZ* basis. Due to the prohibitive computational cost, it was not possible to obtain CCSD(T) PEC's using the full aug-cc-pVDZ basis set. The ΔCCSD(T) correction is computed in an aug-cc-pVDZ* basis as

$$\Delta\mathrm{CCSD(T)} = E_{\mathrm{CCSD(T)}}^{\mathrm{aug-cc-pVDZ^*}} - E_{MP2}^{\mathrm{aug-cc-pVDZ^*}}$$

This correction is combined with the MP2/aug-cc-pVQZ* curves to estimate high-quality CCSD(T)/aug-cc-pVQZ* potential energy curves for the benzene dimer according to the equation

$$E_{\mathrm{CCSD(T)}}^{\mathrm{aug-cc-pVQZ^*}} = E_{MP2}^{\mathrm{aug-cc-pVQZ^*}} + \Delta\mathrm{CCSD(T)}$$

If we compare our current ΔCCSD(T) values evaluated at the same intermonomer distances as the ones used in our previous work[19] for the sandwich, T-shaped, and PD dimer configurations, we find that the two approaches agree to within 0.02 kcal mol^{-1}.

To further elucidate the nature of $\pi-\pi$ interactions in the benzene dimer, potential energy curves were computed using symmetry-adapted perturbation theory (SAPT)[43-45] from their electrostatic, exchange, induction, and dispersion contributions for the sandwich and the T-shaped configurations. In SAPT, the dimer Hamiltonian is composed of three operators as $H = F + W + V$, where F is the Fock operator, representing the sum of the Fock operators for the separate monomers; W is the intramonomer correlation operator, and V is the intermolecular interaction operator. The SAPT interaction energy can be represented as

$$E_{\mathrm{int}} = E_{\mathrm{int}}^{\mathrm{HF}} + E_{\mathrm{int}}^{\mathrm{CORR}}$$

where $E_{\mathrm{int}}^{\mathrm{HF}}$ describes interactions at the Hartree−Fock level and can be represented as

$$E_{\mathrm{int}}^{\mathrm{HF}} = E_{\mathrm{elst}}^{(10)} + E_{\mathrm{exch}}^{(10)} + E_{\mathrm{ind,resp}}^{(20)} + E_{\mathrm{exch-ind,resp}}^{(20)} + \delta E_{\mathrm{int,resp}}^{\mathrm{HF}}$$

The superscripts (*ab*) denote orders in perturbation theory with respect to operators V and W, respectively. The subscripts "resp" indicate that the induction and exchange-induction contributions include the coupled-perturbed Hartree−Fock response.[45] The $\delta E_{\mathrm{int}}^{\mathrm{HF}}$ term contains the third- and higher-order HF induction and exchange-induction contributions.

We have employed the SAPT2 approach in treating the correlated portion of the interaction energy. The correlation energy thus obtained is equivalent to the supermolecular MP2 correlation energy and can be represented as

$$E_{\mathrm{int}}^{\mathrm{CORR}} = E_{\mathrm{elst,resp}}^{(12)} + E_{\mathrm{exch}}^{(11)} + E_{\mathrm{exch}}^{(12)} + {}^tE_{\mathrm{ind}}^{(22)} + {}^tE_{\mathrm{exch-ind}}^{(22)} + E_{\mathrm{disp}}^{(20)} + E_{\mathrm{exch-disp}}^{(20)}$$

where ${}^tE_{\mathrm{ind}}^{(22)}$ represents the part of $E_{\mathrm{ind}}^{(22)}$ that is not included in $E_{\mathrm{ind,resp}}^{(20)}$, and ${}^tE_{\mathrm{exch-ind}}^{(22)}$ is approximated as

$${}^tE_{\mathrm{exch-ind}}^{(22)} \approx E_{\mathrm{exch-ind,resp}}^{(20)} \frac{{}^tE_{\mathrm{ind}}^{(22)}}{E_{\mathrm{ind,resp}}^{(20)}}$$

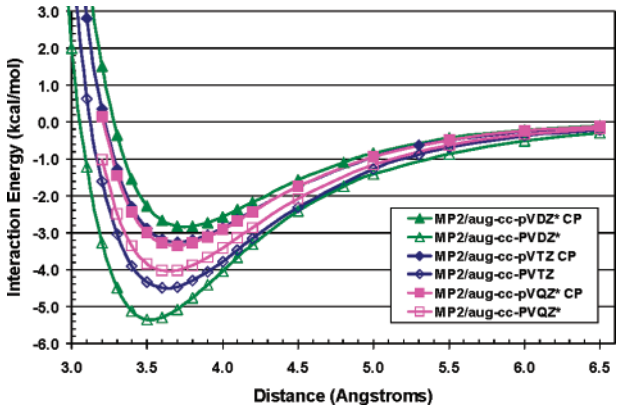

Figure 2. Effect of counterpoise (CP) correction on MP2 potential energy curves for the sandwich configuration of the benzene dimer.

On the basis of the above equations, in this work, we have chosen to express the SAPT2 interaction energy in terms of electrostatic, exchange, induction, and dispersion components as follows:

$$E(\mathrm{electrostatic}) = E_{\mathrm{elst}}^{(10)} + E_{\mathrm{elst,resp}}^{(12)}$$

$$E(\mathrm{exchange}) = E_{\mathrm{exch}}^{(10)} + E_{\mathrm{exch}}^{(11)} + E_{\mathrm{exch}}^{(12)}$$

$$E(\mathrm{induction}) = E_{\mathrm{ind,resp}}^{(20)} + E_{\mathrm{exch-ind,resp}}^{(20)} + \delta E_{\mathrm{int,resp}}^{\mathrm{HF}} + {}^tE_{\mathrm{ind}}^{(22)} + {}^tE_{\mathrm{exch-ind}}^{(22)}$$

$$E(\mathrm{dispersion}) = E_{\mathrm{disp}}^{(20)} + E_{\mathrm{exch-disp}}^{(20)}$$

All SAPT calculations reported here have been carried out using a modified aug-cc-pVDZ basis set, denoted aug-cc-pVDZ′, which lacks all diffuse functions on hydrogen and diffuse *d* functions on carbon. The SAPT computations are very time-consuming, and it was not possible to use larger basis sets. However, we have previously observed that SAPT2/aug-cc-pVDZ′ binding energies compare reasonably well to large basis set CCSD(T) energies because of favorable error cancellation.[46] All supermolecular calculations reported in this work were carried out using Q-Chem 2.0,[47] PSI 3.2,[48] and MOLPRO.[49] SAPT computations were performed using the SAPT2002 program.[43]

Results and Discussion

Basis Set Superposition Error. Theorists and computational chemists often have strong and conflicting opinions about the efficacy of the Boys−Bernardi counterpoise (CP) correction[42] in weakly interacting systems such as the benzene dimer. Dunning[50] has pointed out that the counterpoise correction often leads to a smoother convergence of the interaction energy with respect to basis set, but it can also lead to larger errors for small basis sets. Indeed, this behavior is observed in hydrogen bonded complexes.[51] On the other hand, our prior experience with the benzene dimer shows that the counterpoise-corrected binding energies converge more rapidly with respect to basis set than the uncorrected energies.[19] This is demonstrated again in Figure 1, which displays the MP2 potential energy curves for a series of basis sets, both with and without the counterpoise correction. We will therefore report only counterpoise-corrected results for the remainder of the paper.

Sandwich Configuration. The potential energy curves for the sandwich configuration of the benzene dimer are plotted in Figure 3 along with the ΔCCSD(T) correction. For the

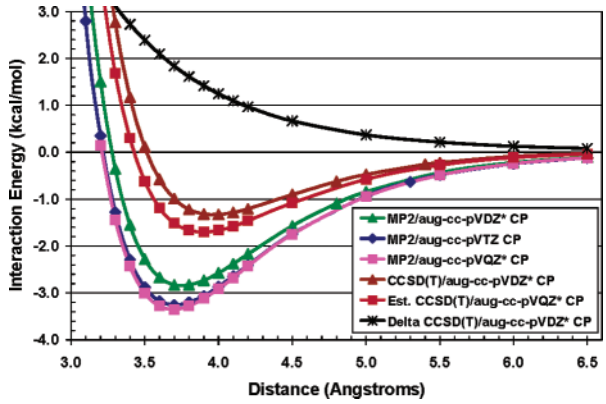

Figure 3. MP2 and CCSD(T) potential energy curves for the sandwich configuration of the benzene dimer. ΔCCSD(T) denotes the difference between CCSD(T) and MP2 (see text). All results reflect counterpoise correction.

TABLE 1: Benzene Dimer Geometries (R in Å)[a]

method	basis	S	T	PD R_1	PD R_2
MP2	aug-cc-pVDZ*[b]	3.8	5.0	3.4	1.6
	aug-cc-pVTZ	3.7	4.9	3.4	1.6
	aug-cc-pVQZ*[c]	3.7	4.9	3.4	1.6
CCSD(T)	aug-cc-pVDZ*	4.0	5.1	3.6	1.8
Estd. CCSD(T)/aug-cc-pVQZ*		3.9	5.0	3.6	1.6

[a] All intermonomer parameters obtained using the best estimates of monomer geometry (C−C = 1.3915, C−H = 1.0800 Å, ref 41). [b] This is an aug-cc-pVDZ basis for carbon and cc-pVDZ for hydrogen. [c] This is an aug-cc-pVQZ basis without g functions on carbon and f functions on hydrogen.

MP2method, the aug-cc-pVTZ and aug-cc-pVQZ* curves are nearly coincident, and they give nearly the same equilibrium intermonomer distances of 3.7 Å. The aug-cc-pVDZ* curve is parallel to the aforementioned curves and gives a slightly larger equilibrium intermonomer distance of 3.8 Å (see Table 1). The aug-cc-pVTZ basis stabilizes the dimer by 0.42 kcal mol^{-1} relative to the much smaller aug-cc-pVDZ* basis at their corresponding minima, with the difference in interaction energies being larger than 1 kcal mol^{-1} at shorter intermonomer distances (3.2 Å or less). The aug-cc-pVQZ* basis stabilizes the dimer by only an additional 0.10 kcal mol^{-1} compared to the aug-cc-pVTZ basis at the corresponding minima and by about 0.2 kcal mol^{-1} at shorter intermonomer distances. This suggests that our high quality MP2/aug-cc-pVQZ* potential energy curves are close to the complete basis set (CBS) limit at the MP2 level.

To better account for electron correlation, the CCSD(T) potential energy curve was computed using the aug-cc-pVDZ* basis set. By computing the ΔCCSD(T) correction in that basis, and adding it to the MP2/aug-cc-pVQZ* results, an estimate of the CCSD(T)/aug-cc-pVQZ* PEC was obtained. It is clear from Figure 3 that ΔCCSD(T) is very large at smaller R (e.g., ΔCCSD(T) = 3.57 kcal mol^{-1} at R = 3.2 Å), and it remains large (1.42 kcal mol^{-1}) at the estimated CCSD(T)/aug-cc-pVQZ* equilibrium geometry (R = 3.9 Å). This confirms earlier observations[16,19,26] that MP2 significantly overbinds compared to CCSD(T). Additionally, the difference between the CCSD(T)/aug-cc-pVDZ* and the estimated CCSD(T)/aug-cc-pVQZ* interaction energies is larger than one kcal mol^{-1} at smaller R and is about 0.4 kcal mol^{-1} at the estimated CCSD(T)/aug-cc-pVQZ* equilibrium geometry.

Our current best estimate of the interaction energy for the sandwich the benzene dimer, evaluated at the equilibrium intermonomer distance (R = 3.9 Å) of the CCSD(T)/aug-cc-pVQZ* PEC, is −1.70 kcal mol^{-1}, which is very close to the estimated complete basis set (CBS) CCSD(T) interaction energy of −1.81 kcal mol^{-1} from our previous work,[19] evaluated at the MP2/aug-cc-pVTZ optimized dimer geometry of R = 3.7 Å (see Table 2).

TABLE 2: Interaction Energies (kcal mol^{-1}) for Different Configurations of the Benzene Dimer[a]

method	basis	S	T	PD
MP2	aug-cc-pVDZ*[b]	−2.83	−3.00	−4.12
	aug-cc-pVTZ	−3.25	−3.44	−4.65
	aug-cc-pVQZ*[c]	−3.35	−3.48	−4.73
	aug-cc-pVQZ[d]	−3.37	−3.54	−4.79
CCSD(T)	aug-cc-pVDZ*	−1.33	−2.24	−2.22
estd. CCSD(T)/aug-cc-pVQZ*		−1.70	−2.61	−2.63
estd. CBS CCSD(T)[d,e]		−1.81	−2.74	−2.78

[a] Unless otherwise noted, all calculations used the optimized dimer geometry at each level of theory, and rigid monomer geometry (C−C = 1.3915, C−H = 1.0800 Å, ref 41). [b] This is an aug-cc-pVDZ basis for carbon and cc-pVDZ for hydrogen. [c] This is an aug-cc-pVQZ basis without g functions on carbon and f functions on hydrogen. [d] At the MP2/aug-cc-pVTZ optimized dimer geometry (ref 19) and using the best estimates of monomer geometry (C−C = 1.3915, C−H = 1.0800 Å, ref 41). [e] See ref 19 for full details.

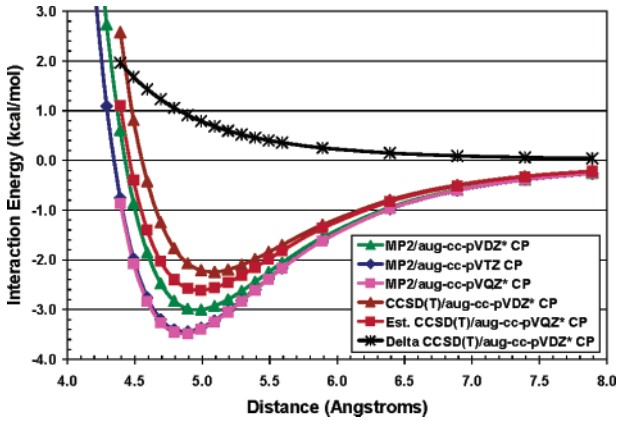

Figure 4. MP2 and CCSD(T) potential energy curves for the T-shaped configuration of the benzene dimer. ΔCCSD(T) denotes the difference between CCSD(T) and MP2 (see text). All results reflect counterpoise correction.

T-Shaped Configuration. The PEC's for the T-shaped configuration of the benzene dimer are plotted in Figure 4 along with the ΔCCSD(T) correction. At the MP2 level, we see that the aug-cc-pVDZ, aug-cc-pVTZ and aug-cc-pVQZ* curves are nearly parallel and give similar equilibrium intermonomer distances of 5.0, 4.9, and 4.9 Å, respectively (see Table 1); indeed, the aug-cc-pVTZ and aug-cc-pVQZ* curves are nearly identical and are hard to distinguish in the figure. By examining Figure 4 and Table 2, we see that at the MP2 level the aug-cc-pVTZ basis stabilizes the dimer by 0.44 kcal mol^{-1} relative to the aug-cc-pVDZ* basis at their corresponding minima; the difference in binding energies is larger at shorter R. The aug-cc-pVQZ* basis stabilizes the dimer by a small 0.04 kcal mol^{-1} compared to the aug-cc-pVTZ basis at equilibrium, again showing that the MP2/aug-cc-pVQZ* curves are very close to the CBS limit at the MP2 level.

The equilibrium intermonomer distances are 5.1 and 5.0 Å at the CCSD(T)/aug-cc-pVDZ* and the estimated CCSD(T)/aug-cc-pVQZ* levels of theory, respectively. This is in good accord with the microwave results of Arunan and Gutowsky,[23] who found a distance of 4.96 Å between the centers of mass of the gas-phase benzene dimer. The difference between the CCSD(T) and the MP2 equilibrium geometries is in agreement

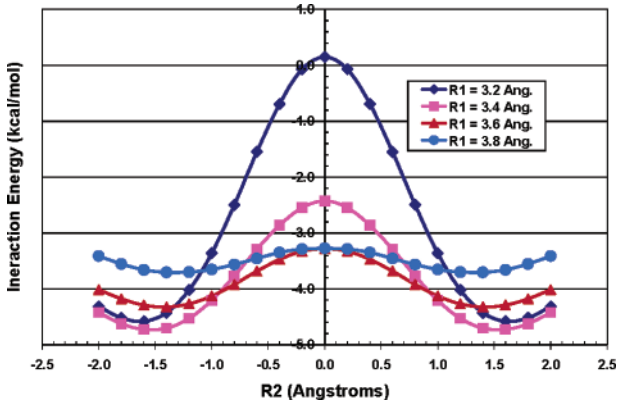

Figure 5. Potential energy curves for the parallel-displaced configuration of the benzene dimer at the (counterpoise-corrected) MP2/aug-cc-pVQZ* level of theory.

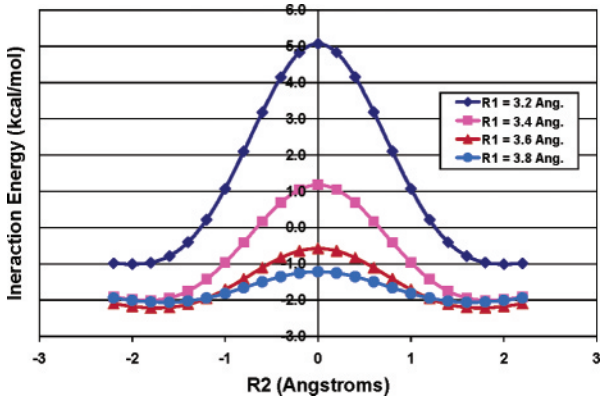

Figure 6. Potential energy curves for the parallel-displaced configuration of the benzene dimer at the (counterpoise-corrected) CCSD(T)/aug-cc-pVDZ* level of theory.

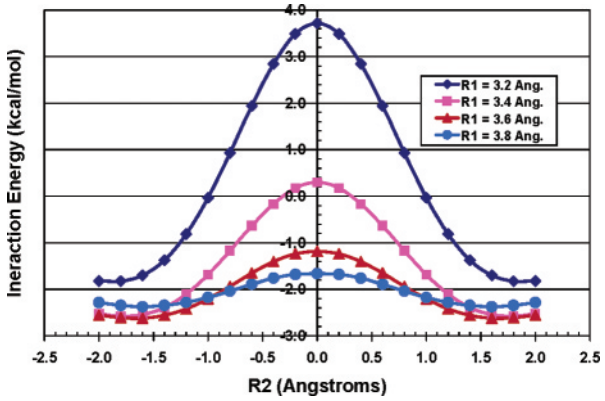

Figure 7. Potential energy curves for the parallel-displaced configuration of the benzene dimer at the (counterpoise-corrected) estimated CCSD(T)/aug-cc-pVQZ* level of theory.

with the trend observed with the sandwich dimer, where the CCSD(T) equilibrium distances were found to be 0.1−0.3 Å larger than the MP2 ones.

The ΔCCSD(T) correction is large for R smaller than the equilibrium distance (e.g., ΔCCSD(T) is about 2 kcal mol^{-1} at R = 4.4 Å). At the estimated CCSD(T)/aug-cc-pVQZ* equilibrium geometry, ΔCCSD(T) is 0.79 kcal mol^{-1}, compared with a much larger value of 1.42 kcal mol^{-1} for the sandwich configuration of the benzene dimer. The reduced importance of higher-order terms in the description of electron correlation for the T-shaped configuration is consistent with the reduced overlap between the monomers in that geometry. The difference between CCSD(T)/aug-cc-pVDZ* and estimated CCSD(T)/aug-cc-pVQZ* values is larger than one kcal mol^{-1} at smaller R, about 0.4 kcal mol^{-1} at equilibrium R = 5.0 Å, and less than 0.1 kcal mol^{-1} for R > 6Å.

Burley and Petsko[4] observed that, in proteins, aromatic side chains separated by distances ranging from 4.5 to 7.0 Å and with dihedral angles near 90° are the most common. Results from our estimated CCSD(T)/aug-cc-pVQZ* curve (see Figure 4) for the T-shaped dimer support the idea that perpendicular interactions are significantly stabilized at these distances. At this level of theory, dimers separated by intermonomer distances larger than 4.5 Å have favorable binding energies, with the binding energy becoming small (<0.4 kcal mol^{-1}) for dimers separated by a distance R greater than 7.0 Å. Our current best estimate of the binding energy for the T-shaped benzene dimer, evaluated at the equilibrium R = 5.0 Å of the CCSD(T)/aug-cc-pVQZ* PEC, gives an interaction energy of −2.61 kcal mol^{-1}, which is only 0.13 kcal mol^{-1} less attractive than the estimated complete basis set (CBS) CCSD(T) interaction energy of −2.74 kcal mol^{-1} from our previous work[19] (see Table 2).

Parallel-Displaced Configuration. Figure 5 presents the potential energy curves for the parallel-displaced configuration of the benzene dimer at the MP2/aug-cc-pVQZ* level of theory (MP2/aug-cc-pVDZ* and MP2/aug-cc-pVTZ PEC's are not displayed). At the MP2 level, the CP-corrected aug-cc-pVDZ*, aug-cc-pVTZ, and aug-cc-pVQZ* curves are nearly parallel and give nearly the same equilibrium intermonomer distances of R_1 = 3.4 Å and R_2 = 1.6 Å (see Table 1), suggesting again that smaller basis sets such as aug-cc-pVDZ* are sufficient for intermonomer geometry optimizations. With regard to the MP2 binding energies, the aug-cc-pVTZ basis stabilizes the dimer by 0.53 kcal mol^{-1} relative to the aug-cc-pVDZ* basis at their corresponding minima, with the aug-cc-pVQZ* basis increasing stabilization at equilibrium by another 0.08 kcal mol^{-1} (see Table 2). As shown in Figures 5−7, the sandwich configuration of the benzene dimer represents a maximum (saddle point) along the horizontal displacement coordinate R_2 which connects two equivalent parallel-displaced configurations.

Figures 6 and 7 display the CCSD(T)/aug-cc-pVDZ* and the estimated CCSD(T)/aug-cc-pVQZ* potential energy curves, respectively (for clarity, the ΔCCSD(T) curves are not shown). In contrast to the MP2 potential energy curves, these two curves are not totally parallel, with equilibrium horizontal displacements of R_2 = 1.8 and 1.6 Å, respectively (the vertical distance R_1 = 3.6 Å is the same for both basis sets).

At the estimated CCSD(T)/aug-cc-pVQZ* equilibrium geometry, ΔCCSD(T) is 1.67 kcal mol^{-1}, with larger values at shorter intermonomer distances. This correction is comparable in size to the sandwich ΔCCSD(T), especially at smaller R_2 values, and is about twice as large as the T-shaped value. The CCSD(T)/aug-cc-pVQZ* equilibrium interaction energy is −2.63 kcal mol^{-1}, again close to the estimated complete basis set (CBS) CCSD(T) interaction energy of −2.78 kcal mol^{-1} from our previous work.[19] This result, combined with those for the sandwich and the T-shaped configurations, indicates that the CCSD(T)/aug-cc-pVQZ* potential energy curves should be accurate to a few tenths of a kilocalorie per mole compared to the ab initio limit.

To confirm the assumption that the ΔCCSD(T) correction is insensitive to the improvement of the basis set, we have performed ΔCCSD(T) calculations for the three benzene dimer configurations using three basis sets, specifically aug-cc-pVDZ* (336 functions), aug-cc-pVDZ (384 functions), and aug-cc-pVTZ minus the f functions on carbon and the d

TABLE 3: Estimates of the ΔCCSD(T) Correction (in kcal mol^{-1}) for Different Configurations of the Benzene Dimer[a]

basis	S	T	PD
aug-cc-pVDZ*[b]	1.84	0.91	2.18
aug-cc-pVDZ	1.83	0.89	2.18
aug-cc-pVTZ(-f/-d)[c]	1.83	0.92	2.21
cc-pVDZ[d]	1.29	0.71	1.43
cc-pVTZ[d]	1.59	0.83	1.79

[a] At the MP2/aug-cc-pVTZ optimized dimer geometry and using the best estimates of monomer geometry (C−C = 1.3915, C−H = 1.0800Å, ref 41). [b] This is an aug-cc-pVDZ basis for carbon and cc-pVDZ for hydrogen. [c] This is an aug-cc-pVTZ basis minus f's on carbon and d's on hydrogen. [d] Reference 18.

TABLE 4: Contributions to the Interaction Energy (kcal mol^{-1}) for Different Configurations of the Benzene Dimer[a,b]

dimer	*E*(elec.)	*E*(exch.)	*E*(ind.)	*E*(disp.)
sandwich	−0.974	6.034	−0.330	−6.527
T-shaped	−2.244	4.866	−0.670	−4.366
parallel-displaced	−2.799	8.652	−0.900	−7.895

[a] At the MP2/aug-cc-pVTZ optimized monomer and dimer geometries as reported in ref 19. [b] At the SAPT2/aug-cc-pVDZ′ level of theory.

functions on hydrogen (540 functions). These calculations were performed at the MP2/aug-cc-pVTZ optimized dimer geometries[19] and using the best estimates of monomer geometry[41] [R(C−C) = 1.3915 Å, R(C−H) = 1.0800 Å]. We can see from Table 3 that ΔCCSD(T) is quite insensitive to basis set improvement as long as the basis set used is augmented with diffuse functions. Neglecting diffuse functions in the basis set results in smaller and less accurate values even if a large basis set is used; our value for ΔCCSD(T) obtained using the aug-cc-pVDZ* basis set (336 functions) is more accurate than that obtained using the larger cc-pVTZ basis set (384 functions) employed in some previous work.[18]

Underlying Fundamental Forces in $\pi-\pi$ Interactions

To explore the contribution of different energy components to the total interaction energy of the benzene dimer, we computed SAPT2/aug-cc-pVDZ′ interaction energies in terms of their electrostatic, exchange, induction, and dispersion components for the sandwich, T-shaped, and parallel-displaced dimer configurations. These calculations were performed at the MP2/aug-cc-pVTZ optimized monomer and dimer geometries from our previous work.[19] Table 4 indicates that the T-shaped dimer has a more stabilizing electrostatic interaction than the sandwich configuration due to favorable quadrupole−quadrupole interactions. The parallel-displaced configuration has the most favorable electrostatic interaction because some of the partially positive hydrogens on each ring are situated on top of the partially negative carbons of the other ring. Also, in the parallel-displaced configuration, the aromatic rings are closer together than in either the sandwich or the T-shaped configurations, and the interpenetration of the electron clouds of the monomers will have a stabilizing effect on the electrostatic interaction. This increased charge overlap also causes the parallel-displaced configuration to have the largest destabilizing exchange-repulsion interaction and the largest stabilizing dispersion interaction, whereas the T-shaped configuration has the smallest exchange-repulsion and the least favorable dispersion interaction. The induction contribution to the binding energy is much smaller than other energy components and is most favorable for the parallel-displaced configuration (−0.90 kcal mol^{-1}), with the sandwich having the least favorable induction

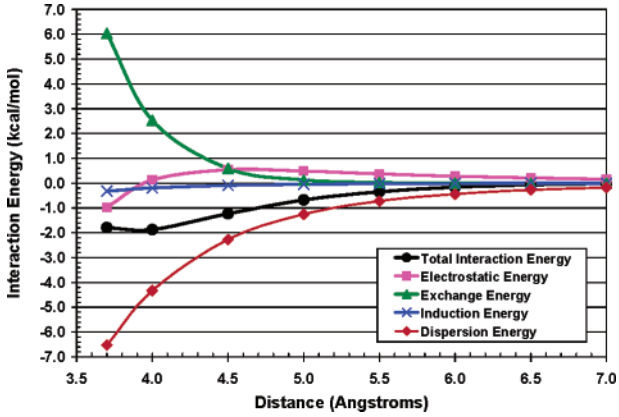

Figure 8. Total binding energy and its electrostatic, exchange, induction, and dispersion components at the SAPT2/aug-cc-pVDZ′ level for the sandwich configuration of the benzene dimer.

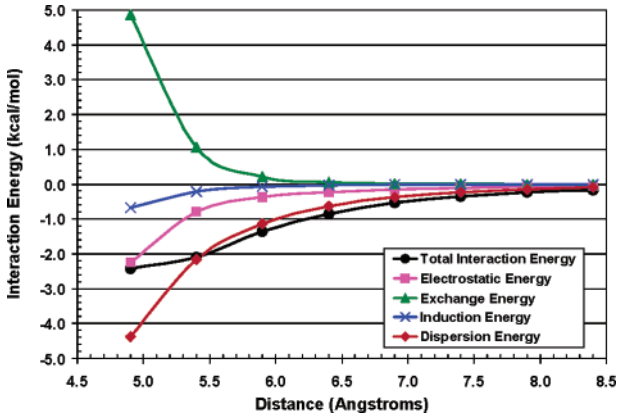

Figure 9. Total binding energy and its electrostatic, exchange, induction, and dispersion components at the SAPT2/aug-cc-pVDZ′ level for the T-shaped configuration of the benzene dimer.

of −0.33 kcal mol^{-1}. It should be noted that the electrostatic energies for the three configurations are reasonably similar to our best coupled-cluster estimates of the total binding energies (although the electrostatic stabilization of the sandwich configuration is only about half the interaction energy). This is consistent with the general success of the Hunter−Sanders rules,[2] which provide qualitative predictions of geometrical effects in $\pi-\pi$ interactions based solely on electrostatic considerations. However, the large variation in the exchange-repulsion and dispersion terms as a function of the dimer configuration cautions against an over-reliance on the electrostatic component for predictions; indeed, we have shown recently that the Hunter−Sanders rules do not correctly predict the energetic order of substituted the benzene dimers.[46]

To better understand the behavior of the different contributions to the energy at different intermonomer distances, we also computed the SAPT2/aug-cc-pVDZ′ energy components at multiple geometries for the sandwich and T-shaped dimer configurations. We can see from Figure 8 for the sandwich configuration that the dispersion energy is the dominating attractive contribution. At distances R > 5.0 Å, the exchange and exchange-corrected induction contributions are negligible, and the electrostatic contribution is small (<0.5 kcal mol^{-1}) and repulsive. For R < 4.0 Å, the exchange-repulsion term is significant and the electrostatic term becomes attractive due to the stabilizing short-range electrostatic penetration resulting from the charge overlap of the electron clouds of the monomers. For the T-shaped the benzene dimer (see Figure 9), even though the dispersion energy is still the dominating attractive contribu-

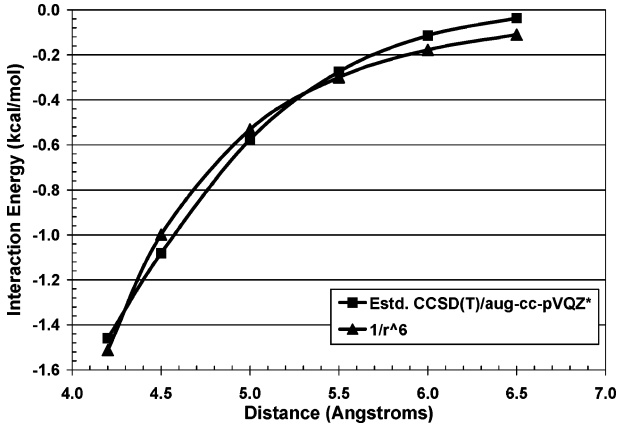

Figure 10. Asymptotic $1/r^6$ fit of the estimated CCSD(T)/aug-cc-pVQZ* potential energy curve for the sandwich configuration of the benzene dimer.

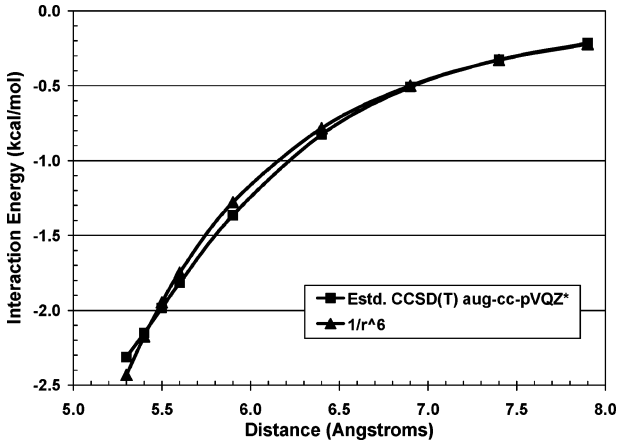

Figure 11. Asymptotic $1/r^6$ fit of the estimated CCSD(T)/aug-cc-pVQZ* potential energy curve for the T-shaped configuration of the benzene dimer.

tion, there is also a stabilizing electrostatic contribution at all intermonomer distances due to favorable quadrupole−quadrupole interactions. As for the sandwich case, the exchange and induction contributions are negligible at large intermonomer distances.

Since the potential of the dominating dispersion interaction falls off with distance as $1/R$,[6] we performed a least-squares fit of the tail of the potential energy curve for the sandwich and T-shaped configurations using the equation $\Delta E = -B/R^6$, where B is a constant to be determined from the fit. In both cases, we included points with R as small as ∼0.5 Å beyond equilibrium. For the sandwich the benzene dimer, we have fitted the estimated CCSD(T)/aug-cc-pVQZ* curve from $R = 4.2$ to 6.5 Å (see Figure 10) and obtained a B value of 8.3×10^3 kcal mol^{-1} Å^6. Similarly, for the T-shaped dimer, we have fitted the estimated CCSD(T)/aug-cc-pVQZ* curves from $R = 5.3$ to 7.9 Å (see Figure 11) and obtained a B value of 5.39×10^4 kcal mol^{-1} Å^6. The imperfect $1/R^6$ fit displayed in the figures results from the fact that in addition to dispersion other energy components (such as electrostatic and exchange-repulsion) contribute to the overall binding energy, especially at the shorter intermonomer distances.

Conclusions

In this work, we have generated high-quality potential energy curves for the sandwich, T-shaped, and parallel-displaced configurations of the simplest prototype of aromatic $\pi-\pi$ interactions, the benzene dimer. At the MP2 level, the aug-cc-pVTZ and aug-cc-pVQZ* (truncated aug-cc-pVQZ) basis sets are much larger than previous basis sets used to compute potential energy curves (PEC's) for the benzene dimer. Although equilibrium geometries can be accurately predicted using smaller basis sets at the MP2 level, the binding energies are sensitive to the improvement of the basis set. Therefore, large basis sets (of quadruple-ζ quality or better) are needed to ensure convergence within a few tenths of one kcal mol^{-1} of the MP2 complete basis set (CBS) limit. By combining the MP2/aug-cc-pVQZ* results with a correction for the difference between the CCSD(T) and MP2 interaction energies [the ΔCCSD(T) correction] determined in a smaller basis, estimates of the CCSD(T)/aug-cc-pVQZ* potential energy curves were obtained, which should be within a few tenths of one kcal mol^{-1} of the ab initio limit. The ΔCCSD(T) correction is large at distances around or shorter than the equilibrium distance but dies off to zero at large distances, and it leads to larger intermonomer distances in the equilibrium geometries by 0.1−0.3 Å compared to the MP2 method. For the T-shaped dimer, the equilibrium intermonomer distance of 5.0 Å is in good accord with the microwave results of Arunan and Gutowsky[23] (4.96 Å) and with the observed mean distance of 5.05 Å between the phenyl ring centroids for interacting aromatic side chains in proteins.[4]

Our SAPT analysis of the binding energies reveals that dispersion is the dominant stabilizing contribution to the total binding energy, but electrostatics are also stabilizing for all three configurations at their equilibrium geometries. Electrostatics become destabilizing at larger distances for the sandwich configuration, but they remain stabilizing at all distances for the T-shaped configuration due to a favorable quadrupole−quadrupole interaction. Both induction and exchange-repulsion interactions are negligible at large intermonomer distances, with the exchange-repulsion becoming significant near equilibrium. Because dispersion dominates at large distances, the tails of the potential energy curves for the sandwich and T-shaped configurations are well described by a function of the form $-B/R^6$, even when points close to equilibrium are included in the fit.

Very few high-quality potential energy curves are currently available for weakly interacting systems. The present curves for the benzene dimer will aid the development of new force-field and density functional methods that are computationally inexpensive and capable of modeling $\pi-\pi$ interactions in biomolecules.

Acknowledgment. C.D.S. is a Blanchard Assistant Professor of Chemistry at Georgia Tech and acknowledges a Camille and Henry Dreyfus New Faculty Award and an NSF CAREER award (Grant No. CHE-0094088). The Center for Computational Molecular Science and Technology is funded through a Shared University Research (SUR) grant from IBM and by Georgia Tech. We gratefully acknowledge partial support by the Molecular Design Institute at Georgia Tech, under Prime Contract N00014-95-1-1116 from the Office of Naval Research.

Supporting Information Available: Cartesian coordinates and potential energy curves of dimers. This material is available free of charge via the Internet at http://pubs.acs.org

References and Notes

(1) Mulliken, R. S. *J. Am. Chem. Soc.* **1952**, *74*, 811.
(2) Hunter, C. A.; Sanders, J. K. M. *J. Am. Chem. Soc.* **1990**, *112*, 5525.
(3) Kumph, R. A.; Dougherty, D. A. *Science* **1993**, *261*, 1708.
(4) Burley, S. K.; Petsko, G. A. *Science* **1985**, *229*, 23.

(5) Hunter, C. A.; Singh, J.; Thornton, J. M. *J. Mol. Biol.* **1991**, *218*, 837.
(6) Lerman, L. S. *J. Mol. Biol.* **1961**, *3*, 18.
(7) Saenger, W. *Principles of Nucleic Acid Structure*; Springer-Verlag: New York, 1984.
(8) Zimm, B. H. *J. Chem. Phys.* **1960**, *33*, 1349.
(9) Crothers, D. M.; Zimm, B. H. *J. Mol. Biol.* **1967**, *9*, 1.
(10) Hunter, C. A. *Chem. Soc. Rev.* **1994**, *23*, 101.
(11) Kryger, G.; Silman, I.; Sussman, J. L. *J. Physiol.* **1998**, *92*, 191.
(12) Claessens, C. G.; Stoddart, J. F. *J. Phys. Org. Chem.* **1997**, *10*, 254.
(13) Glaser, R.; Dendi, L. R.; Knotts, N.; Barnes, C. L. *Cryst. Growth Des.* **2003**, *3*, 291.
(14) Lehn, J.,-M. *Supramolecular Chemistry: Concepts and Perspectives*; VCH: New York, 1995.
(15) Tsuzuki, T.; Uchimaru, T.; Tanabe, K. *J. Mol. Struct. (THEOCHEM)* **1994**, *307*, 107.
(16) Hobza, P.; Selzle, H. L.; Schlag, E. W. *J. Phys. Chem.* **1996**, *100*, 18790.
(17) Tsuzuki, S.; Luthi, H. P. *J. Chem. Phys.* **2001**, *114*, 3949.
(18) Tsuzuki, S.; Honda, K.; Uchimaru, T.; Mikami, M.; Tanabe, K. *J. Am. Chem. Soc.* **2002**, *124*, 104.
(19) Sinnokrot, M. O.; Valeev, E. F.; Sherrill, C. D. *J. Am. Chem. Soc.* **2002**, *124*, 10887.
(20) Sinnokrot, M. O.; Sherrill, C. D. *J. Phys. Chem. A* **2003**, *107*, 8377.
(21) Steed, J. M.; Dixon, T. A.; Klemperer, W. *J. Chem. Phys.* **1979**, *70*, 4940.
(22) Law, K. S.; Schauer, M.; Bernstein, E. R. *J. Chem. Phys.* **1984**, *81*, 4871.
(23) Arunan, E.; Gutowsky, H. S. *J. Chem. Phys.* **1993**, *99*, 4294.
(24) Venturo, V. A.; Felker, P. M. *J. Chem. Phys.* **1993**, *99*, 748.
(25) Felker, P. M.; Maxton, P. M.; Schaeffer, M. W. *Chem. Rev.* **1994**, *94*, 1787.
(26) Jaffe, R. L.; Smith, G. D. *J. Chem. Phys.* **1996**, *105*, 2780.
(27) Tsuzuki, S.; Uchimaru, T.; Sugawara, K.; Mikami, M. *J. Chem. Phys.* **2002**, *117*, 11216.
(28) Hobza, P.; Selzle, H. L.; Schlag, E. W. *J. Am. Chem. Soc.* **1994**, *116*, 3500.
(29) Špirko, V.; Engkvist, O.; Slodán, P.; Selzle, H. L.; Schlag, E. W.; Hobza, P. *J. Chem. Phys.* **1999**, *111*, 572.
(30) Kutzelnigg, W.; Klopper, W. *J. Chem. Phys.* **1991**, *94*, 1985.
(31) Murphy, R. B.; Beachy, M. D.; Friesner, R. A.; Ringnalda, M. N. *J. Chem. Phys.* **1995**, *103*, 1481.
(32) Kaminski, G. A.; Stern, H. A.; Berne, B. J.; Friesner, R. A.; Cao, Y. X.; Murphy, R. B.; Zhou, R.; Halgren, T. A. *J. Comput. Chem.* **2002**, *23*, 1515.
(33) Kaminski, G. A.; Stern, H. A.; Berne, B. J.; Friesner, R. A. *J. Phys. Chem. A.* **2004**, *108*, 621.
(34) Liu, Y. P.; Kim, K. S.; Berne, B. J.; Friesner, R. A.; Rick, S. W. *J. Chem. Phys.* **1998**, *108*, 4739.
(35) Yin, D.; MacKerrel, A. D., Jr. *J. Comput. Chem.* **1998**, *19*, 334.
(36) Tsuzuki, S.; Uchimaru, T.; Tanabe, K. *J. Phys. Chem.* **1994**, *98*, 1830.
(37) Grimme, S. *J. Comput. Chem.* **2004**, *25*, 1463.
(38) Goddard, W. A.; Xu, X. *Proc Natl Acad Sci U.S.A.* **2004**, *101*, 2673.
(39) von Lilienfeld, O. A.; Tavernelli, I.; Rothlisberger, U.; Sebastiani, D. submitted.
(40) Kendall, R. A.; Dunning, T. H.; Harrison, R. J. *J. Chem. Phys.* **1992**, *96*, 6796.
(41) Gauss, J.; Stanton, J. F. *J. Phys. Chem. A* **2000**, *104*, 2865.
(42) Boys, S. F.; Bernardi, F. *Mol. Phys.* **1970**, *19*, 553.
(43) Bukowski, R.; Cencek, W.; Jankowski, P.; Jeziorski, B.; Jeziorska, M.; Kucharski, S. A.; Misquitta, A. J.; Moszynski, R.; Patkowski, K.; Rybak, S.; Szalewicz, K.; Williams, H. L.; Wormer, P. E. S. In *SAPT2002: An Ab Initio Program for Many-Body Symmetry-Adapted Perturbation Theory Calculations of Intermolecular Interaction Energies. Sequential and Parallel Versions*. see: http://www.physics.udel.edu/∼szalewic/SAPT/SAPT.html.
(44) Jeziorski, B.; Moszynski, R.; Szalewicz, K. *Chem. Rev.* **1994**, *94*, 1887.
(45) Williams, H. L.; Szalewicz, K.; Jeziorski, B.; Moszynski, R.; Rybak, S. *J. Chem. Phys.* **1993**, *98*, 1279.
(46) Sinnokrot, M. O.; Sherrill, C. D. *J. Am. Chem. Soc.* **2004**, *126*, 7690.
(47) Kong, J.; White, C. A.; Krylov, A. I.; Sherrill, C. D.; Adamson, R. D.; Furlani, T. R.; Lee, M. S.; Lee, A. M.; Gwaltney, S. R.; Adams, T. R.; Daschel, H.; Zhang, W.; Korambath, P. P.; Ochsenfeld, C.; Gilbert, A. T. B.; Kedziora, G. S.; Maurice, D. R.; Nair, N.; Shao, Y.; Besley, N. A.; Maslen, P. E.; Dombroski, J. P.; Baker, J.; Byrd, E. F. C.; Voorhis, T. V.; Oumi, M.; Hirata, S.; Hsu, C.-P.; Ishikawa, N.; Florian, J.; Warshel, A.; Johnson, B. G.; Gill, P. M. W.; Head-Gordon, M.; Pople, J. A. *J. Comput. Chem.* **2000**, *21*, 1532.
(48) Crawford, T. D.; Sherrill, C. D.; Valeev, E. F.; Fermann, J. T.; King, R. A.; Leininger, M. T.; Brown, S. T.; Janssen, C. L.; Seidl, E. T.; Kenny, J. P.; Allen, W. D. In *PSI 3.2*, 2003. See: http://www.psicode.org.
(49) Amos, R. D.; Bernhardsson, A.; Berning, A.; Celani, P.; Cooper, D. L.; Deegan, M. J. O.; Dobbyn, A. J.; Eckert, F.; Hampel, C.; Hetzer, G.; Knowles, P. J.; Korona, T.; Lindh, R.; Lloyd, A. W.; McNicholas, S. J.; Manby, F. R.; Meyer, W.; Mura, M. E.; Nicklass, A.; Palmieri, P.; Pitzer, R.; Rauhut, G.; Schütz, M.; Schumann, U.; Stoll, H.; Stone, A. J.; Tarroni, R.; Thorsteinsson, T.; Werner, H.-J. In *MOLPRO, a package of ab initio programs designed by Werner, H.-J.; Knowles, P. J. Version 2002*. See: http://www.molpro.net.
(50) Dunning, T. H. *J. Phys. Chem. A* **2000**, *104*, 9062−9080.
(51) Halkier, A.; Klopper, W.; Helgaker, T.; Jørgensen, P.; Taylor, P. R. *J. Chem. Phys.* **1999**, *111*, 9157−9167.